Outcrop permeabilities within four facies of a single depositional parasequence, upper San Andres Formation (Permian, Guadalupian/Leonardian), Lawyer Canyon, Guadalupe Mountains, Otero County, New Mexico

Malcolm A. Ferris, Charles Kerans, and Sharp, John M., Jr., 1993, pp. 205-210

in:

Carlsbad Region (New Mexico and West Texas), Love, D. W.; Hawley, J. W.; Kues, B. S.; Austin, G. S.; Lucas, S. G.; [eds.], New Mexico Geological Society 44th Annual Fall Field Conference Guidebook, 357 p.

This page is intentionally left blank to maintain order of facing pages.

OUTCROP PERMEABILITIES WITHIN FOUR FACIES OF A SINGLE DEPOSITIONAL PARASEQUENCE, UPPER SAN ANDRES FORMATION (GUADALUPIAN/LEONARDIAN), LAWYER CANYON, GUADALUPE MOUNTAINS, OTERO COUNTY, NEW MEXICO

MALCOLM A. FERRIS[1], CHARLES KERANS[2] and JOHN M. SHARP, JR.[1]
[1]Department of Geological Sciences, University of Texas at Austin, Austin, Texas 78712; [2]Texas Bureau of Economic Geology, P.O. Drawer X, Austin, Texas 78713-7508

Abstract Permeability was measured on the upper San Andres Formation (Guadalupian/ Leonardian) outcrop in the Lawyer Canyon area of the Algerita Escarpment, Guadalupe Mountains, Otero County, New Mexico. The study area is a 2613-ft horizontal and 15- to 25-ft vertical section consisting of a single mudstone-bounded carbonate parasequence within the transgressive shelf margin. Four genetic facies were identified within the parasequence: (I) a mud-dominated deep-water flooded shelf; (2) a coarsening-upward, mud-supported ooid and peloid wackestone/packstone shallow shelf; (3) an ooid and peloid, grain-supported bar crest; and (4) an ooid and peloid, grain-supported, coarsening-upward bar flank. Data were collected in the field, with a minipermeameter and in the laboratory, on core plugs from the outcrop. Sampling was performed at 769 locations along 31 vertical transects and in two small-scale orthogonal grid patterns. Separation distances varied from 325 feet between the widest space vertical transects, down to a I-in. separation within the smallest scale grid. Experimental variograms computed for the facies data exhibited a proportionately high nugget-to-sill ratio of poorly developed spherical models. Interpretation of correlation range values in vertical variograms indicate a development of vertical variability within the parasequence, from 13 ft to 2 in. Horizontal variogram analysis for correlation range values indicate a scale dependency based on the sample separation and related variogram lag (h). Horizontal variogram ranges are 253 ft and 748 ft for a lag, h, of 100 ft, 22 ft for h of 10 ft, 4 ft for h of 1 ft and 8 in. for h of I in. An intrinsic test for a power-law function showed that the permeability data exhibit a random or "white noise" relationship for different horizontal variogram search distances. A fractal codimension of 0.07 was calculated, which is an order of magnitude below expectations established for other natural phenomena.

INTRODUCTION

The Permian (Leonardian-Guadalupian) San Andres Formation is a prolific reservoir rock in the Permian Basin. Predictions of secondary or tertiary oil recovery in this carbonate reservoir have proven difficult. Consequently, studies by the Texas Bureau of Economic Geology, among others, have investigated the details of permeability and porosity distributions on outcrops and their extrapolation to subsurface conditions. Such data are necessary input into numerical models of enhanced oil recovery (e.g., Dagan, 1986; Weber, 1986; Kerans et al., 1991) or ground-water flow and transport. Recent studies on field permeabilities have included welded tuffs (Fuller and Sharp, 1992; Sharp et al., 1993), fluvial sandstones (Davis and Phillips, 1990), Paleozoic fluvial/deltaic sandstones (Fu et al., 1992) and aeolian sandstones (Chandler et al., 1989).

The ability to obtain accurate permeability data rapidly on cores or outcrops is required to develop geostatistical models of reservoir properties. Air minipermeameters have proven an ideal tool for obtaining such data.

GEOLOGIC SETTING

The San Andres Formation outcrop selected for permeability analysis is on the Algerita Escarpment of the Guadalupe Mountains. This was based upon outcrop accessibility, proximity to producing fields in the San Andres Formation and promising pilot studies by Hinrichs et al. (1986) and Kittridge (1988).

San Andres reservoirs are typically in shallow-water platform-top and upper-slope carbonates with laterally extensive facies and generally low recovery efficiencies (Galloway et al., 1983). The site selected in Lawyer Canyon had exposures of a scale comparable to producing fields. In this study, the area of data collection was confined to a single parasequence as defined by Van Wagoner et al. (1988), a single cycle of genetically related and flood-bounded bed sets. This limitation allows a significant number of measurements to be collected at various vertical and lateral separations within each interpreted genetic facies of the parasequence.

King (1942, 1948) and Hayes (1964) provided early descriptions of the Guadalupe Mountains. First identified by Lee (1909), the San Andres Formation is part of a Permian platform composed of stacked upward-coarsening carbonate cycles on the margins of the Delaware and Mid land Basins. More recent discussions of the local geology are provided by Silver and Todd (1969), Leary (1984), Sarg and Lehmann (1986) and Kerans et al. (1991). The sequence stratigraphy for the San Andres Formation in the Guadalupe mountains was outlined by Kerans et al. (1991), from which a simplified geologic cross section of the San Andres Formation in Lawyer Canyon is taken (Fig. 1).

Permeability measurements were taken from within the basal parasequence of the upper third-order San Andres sequence. This parasequence was mapped in detail by Kerans and Nance (1989, written comm.) and is subdivided into four facies. Facies I is a low-energy, flooded-shelf, sheet-like mudstone bed that thickens downdip from 5 ft in the north to up to 13 ft in the south. This massive facies lacks laminations, perhaps because of bioturbation or subsequent diagenesis, which resulted in recrystallization of the fine mud grains to dolomite microspar. In the outcrop, this facies is fractured at a variety of scales. Many of the smaller fractures are filled by calcite or dolomite.

Facies 2 is a laterally discontinuous, low-energy, draped, shallow-shelf deposit that overlies Facies 1. Facies 2 grades upward from a mudstone and wackestone to a peloid packstone/grain-dominated packstone. Thickness varies from 2 to 6 ft and pinches out between sections Al 1 and A 13 (Fig. 2). This facies contains wavy laminations interspersed with more massive zones that show signs of bioturbation. Dolomite microspar replaces and overprints the original texture. Intracrystalline porosity is observed in these sections (Ferris, 1993, fig. 11B).

Facies 3 is a high-energy, shallow-shelf, ooid-rich grainstone interpreted as a bar crest deposit. This facies caps the mud-rich facies in the northern end of the section (Al—A 11). Facies 3 pinches out at the southern end (A19—A20). This facies exhibits trough cross-stratification and planar-tabular stratifications, which indicate reworking by wave and tidal currents. The fabric is largely replaced by dolomitic microspar.

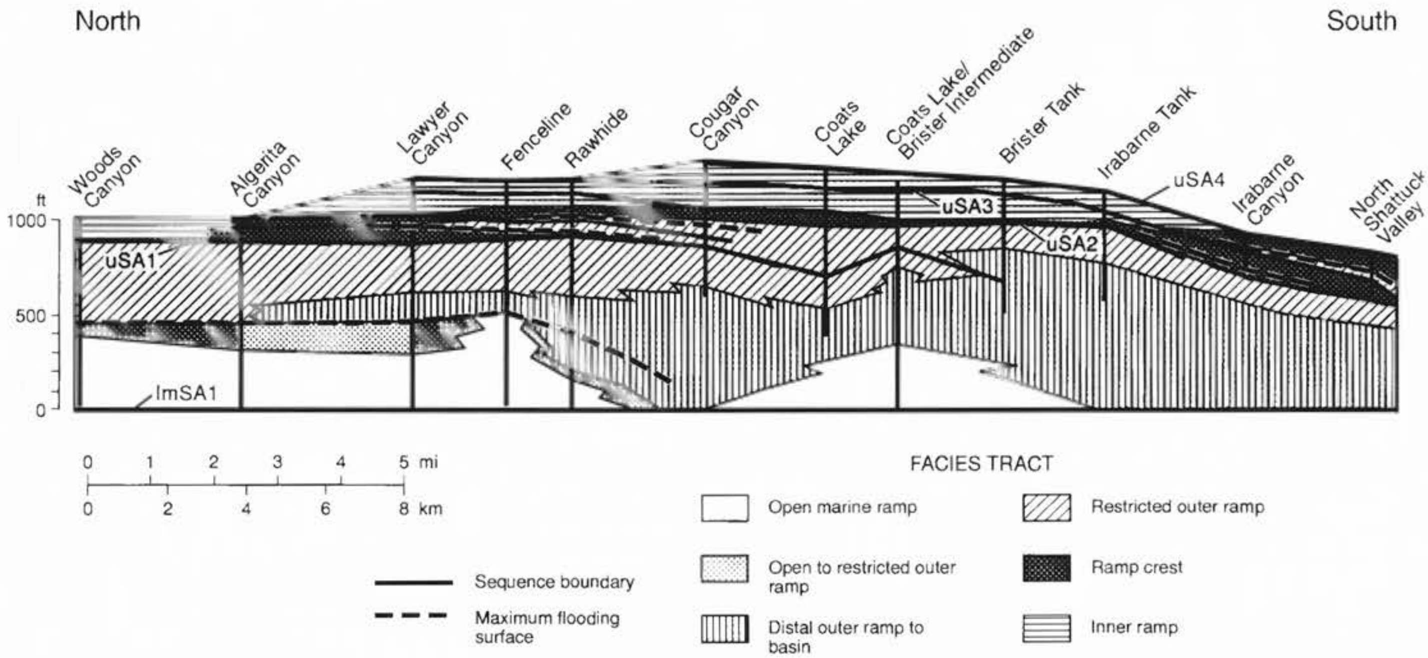

FIGURE 1. Simplified geologic cross section of the San Andres Formation along the Algerita escarpment (from Kerans et al., 1991).

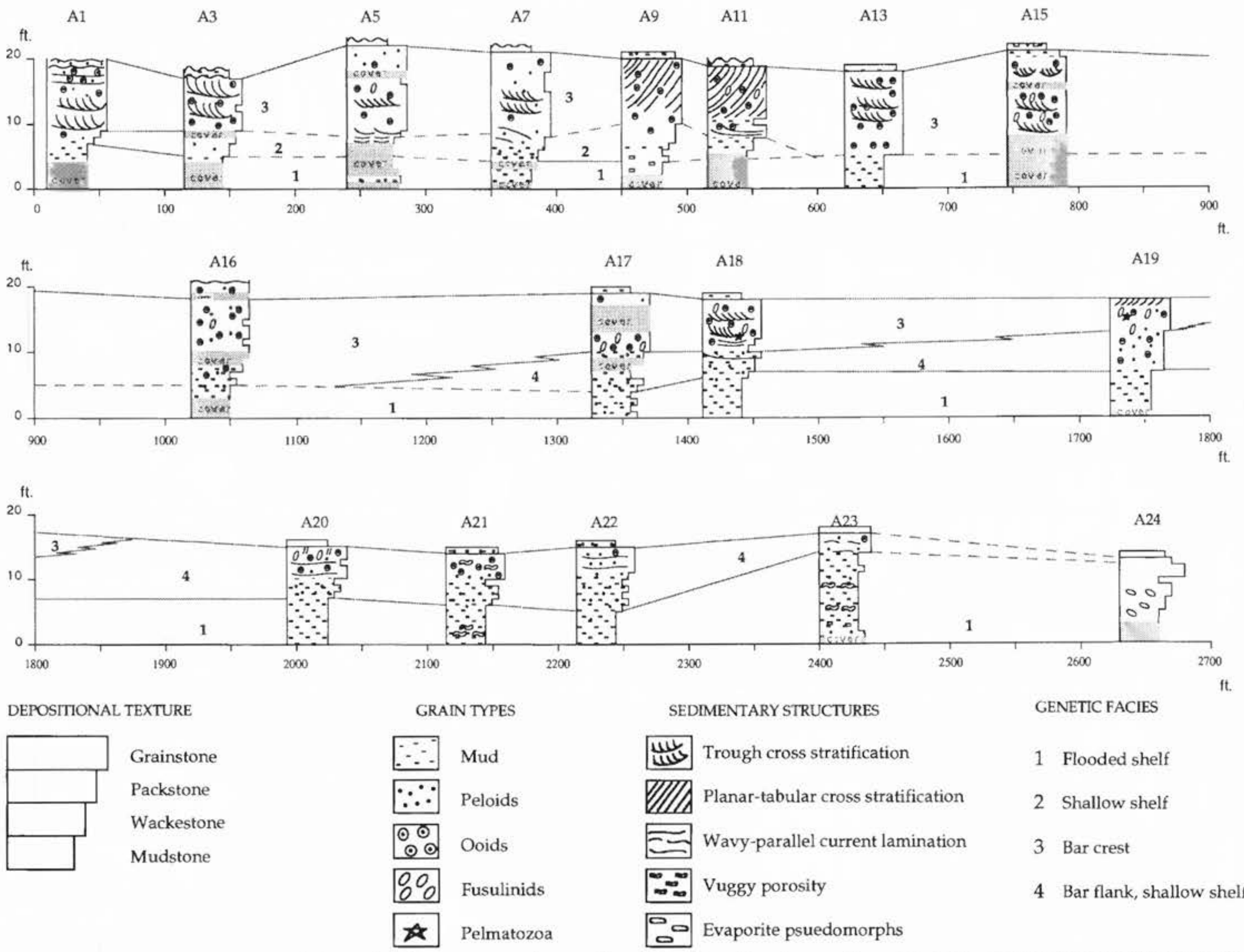

FIGURE 2. Original 16 measured geologic sections in parasequence 1, upper San Andres Formation, Lawyer Canyon study site, as mapped by Kerans and Nance (1989, unpublished). Depositional texture, grain types and sedimentary structures shown with interpretations of genetic-facies lateral continuity.

Primary porosity is retained, but dissolution and cementation disrupt the grain-dominated fabric and fill some of the primary pores and fractures.

Facies 4 is a low-energy, shallow-water, shelf facies, of packstone and wackestone textures. It is transitional between Facies 2 and 3 and is interpreted as a bar-flank deposit. A gradual transition occurs upwards from a mud- to a grain-dominated facies, typified by increasing grain size. The deposits show intermittently preserved, wavy to parallel laminations. Replacement of the fabric by dolomite microspar caused an increase in the intercrystalline porosity of the mud-supported fabric but did not change the interparticle porosity (Ferris, 1993, fig. 11D). For more detailed discussion of the facies, the reader should consult Kerans et al. (1991) or Ferris (1993).

DATA COLLECTION

Permeability data were collected with a mechanical field permeameter (MFP) and augmented by permeabilities estimated from core plugs. Permeabilities were calculated from steady-state flow and pressure values as recorded from flow tubes and dial gauges, respectively, on the device. The MFP was described by Goggin et al. (1988) based upon published designs for air flow permeameters (Dykstra and Parsons, 1950; Eijpe and Weber, 1971).

In this study, the weathering rind was chiseled off the outcrop at measuring points and the permeameter nozzle positioned inside the chiseled area. This avoided problems described by Kittridge (1988) and Ferris (1993). A set of three to five measurements was taken at each point for redundancy.

The permeability data were collected in four distinctly scaled grids, incorporating the measured geologic sections provided by Kerans et al. (1991) and covering an outcrop of the first parasequence for almost half a mile. Sample grids ranged from the largest, Grid A, which considered the entire lateral distance of the study area, to Grid D, which is a 2- by 4-ft outcrop of Facies 3 sampled at a 1-in. scale. All data are contained in Ferris (1993, Appendix A) and the permeabilities were calculated using the equation of Goggin (1988).

RESULTS

Permeability data were contoured (Fig. 3) for the largest grid (Grid A) and analyzed using geostatistical theory. Fig. 3 is a kriged contour map of permeabilities over the outcrop delineated in Fig. 2. In general, the population of MFP-measured permeabilities has a log-normal distribution (Fig. 4). Two major regions are delineated, one of low (<10 md) permeabilities, which is overlain by regions of higher (10-100 md) permeabilities. The former region corresponds to Facies 1, the mud-dominated facies. The bed of mud-dominated fabric at the bottom of this, and presumably other parasequences, indicate their importance in channeling fluid flow. Laterally continuous zones or "streaks" of higher (>100 md) permeability with dimensions of 35 to 376 ft (Fig. 3) were observed to be disrupted and less continuous in the finer-scaled grid sampling.

Geostatistical analysis follows techniques developed by Krige (1943) for estimation of ore reserves and subsequently extended for hydrogeology by many workers (e.g., Fogg, 1986; Gelhar, 1986). Our goal in this analysis is to determine the spatial correlation structure of per-

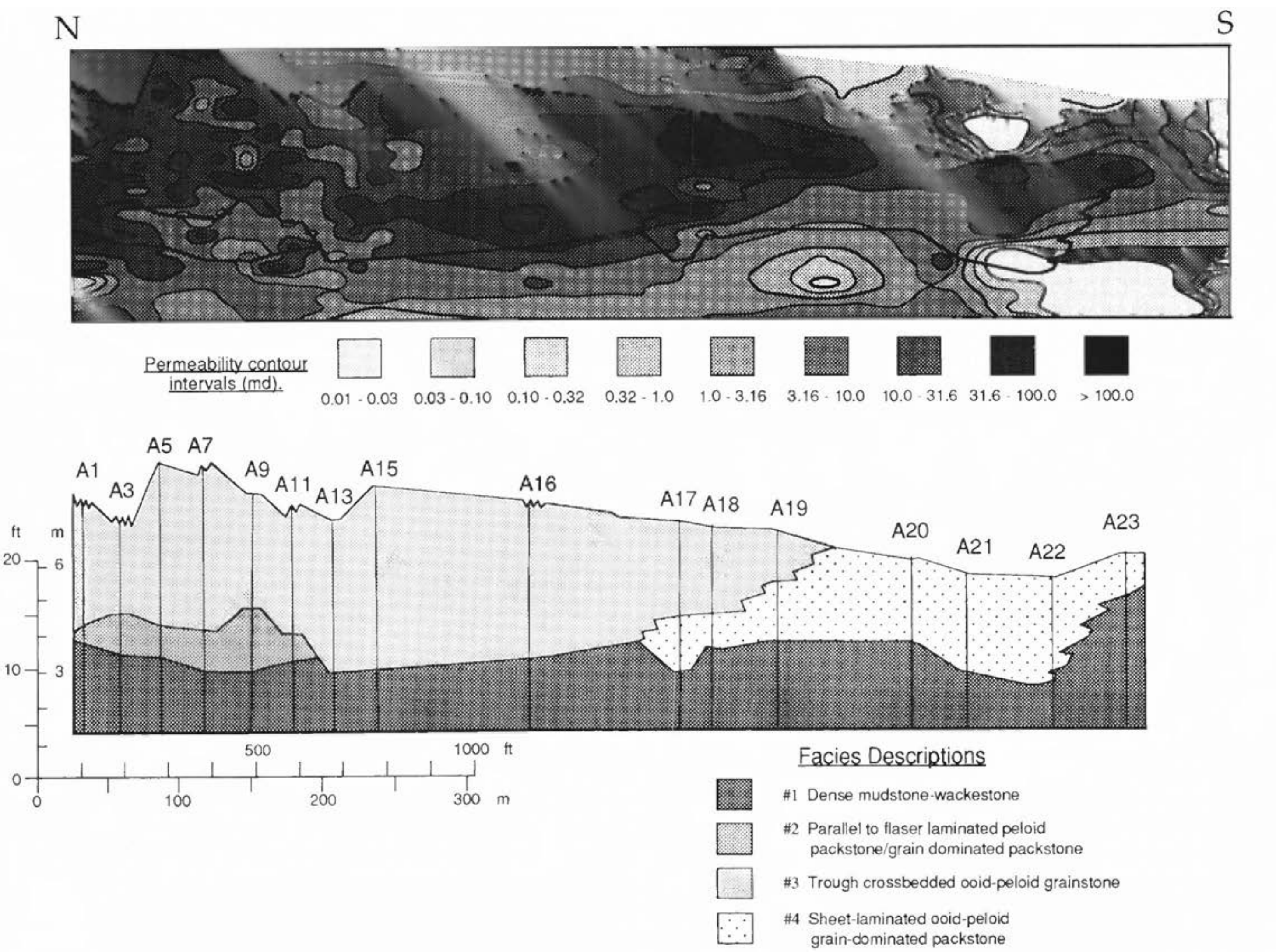

FIGURE 3. Contoured permeability diagram shown with corresponding facies boundaries and descriptions for cross section of study area.

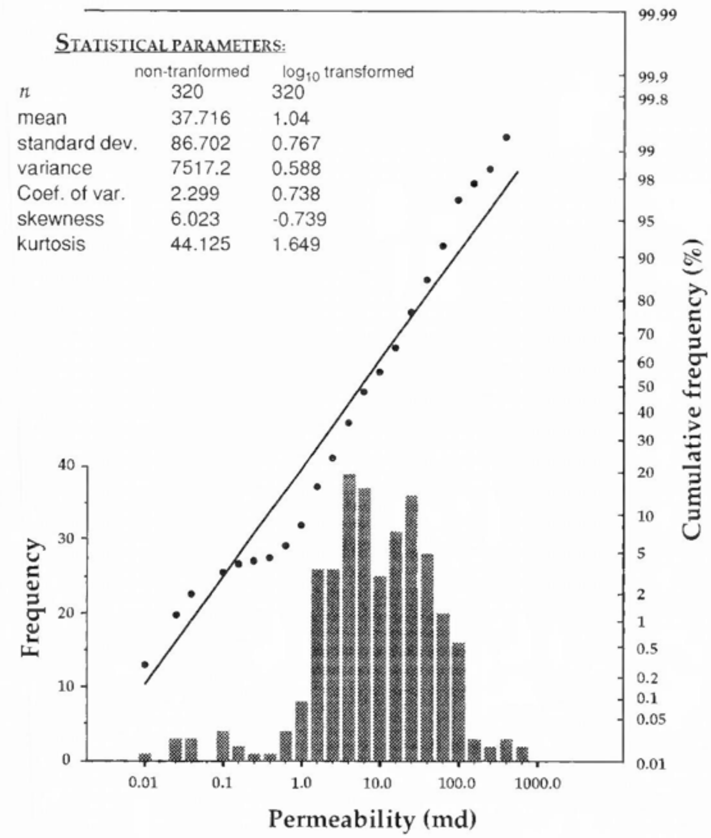

FIGURE 4. Frequency histogram and probability plot graphs for GRID A sample data example. Data shown to exhibit lognormal distribution with exception in the low-permeability range, which is below detection limits of the MFP. The negative and relatively high coefficient of skewness corresponds to this observed deviation from lognormality.

meabilities (i.e., if we know the permeability at one point, how well can we predict its value some distance away?).

For this purpose we used a variogram analysis, plotting variance of data separated by equal distances (or lags) (for details of the analysis, see Ferris, 1993). Both horizontal and vertical variograms were constructed for all four grids (scales of 100 ft, 10 ft, 1 ft and 1 in.). Variogram parameters are given in Table 1. Data for Grid A show a nested, horizontal correlation structure with permeabilities correlated at ranges of 254 and 748 ft. Grid B has a range of 22 ft. For both Grid A and Grid B, the vertical correlation ranges are much less, which reflects the effects of bedding inhomogeneity. Grid C (I-ft sample grid), on the other hand, shows equal correlation structure vertically and horizontally. Grid C was confined to Facies 3, suggesting that this facies is relatively homogeneous. Grid D data, like those for Grids A and B, show greater ranges horizontally, suggesting a structure at scales of less than 1 ft.

The nugget (the inherent heterogeneity at any point) was remarkably consistent at all scales. This indicates that the inherent randomness (or white noise) of the permeability may be due to diagenetic effects that cross facies (fracturing and pore-filling by carbonate cements). Application of power-law theory to the scale-based variograms resulted in a superpositioned variogram (Fig. 5). Calculation of the best-fit line through the points had a slope of 0.155 and a y-intercept (the characteristic variance) of —0.761. Based on the power-law equation of $g = g(0)$ the slope corresponds to the fractal codimension for the population of permeability data and the y-intercept corresponds to the characteristic variance of the population for a baseline lag distance (analogous to the nugget and calculated for h = 1 ft for simplication, since log(1) = 0). Therefore, the fractal codimension **(**1-1**)** is found to be equal to 0.07, an order of magnitude lower than that suggested by Hewett and Berhens (1990) and Mandelbrot (1983) for natural phenomena.

TABLE 1. Variogram results for scale-based sample grids.

Sample	Horizontal (θ = 0°)	Vertical (θ = 90°)
GRID A (100-foot scale)		
nugget ($C_{(0)}$)	0.2	0.16
range ($r_{(1)}$)	253.5 feet	13.0 feet
sill ($C_{(1)}$)	0.305	0.95
range ($r_{(2)}$)	748.3 feet	N.A.
sill ($C_{(2)}$)	0.497	N.A.
GRID B (10-foot scale)		
nugget ($C_{(0)}$)	0.32	0.2
range ($r_{(1)}$)	22.2 feet	4.0 feet
sill ($C_{(1)}$)	0.57	0.44
range ($r_{(2)}$)	N.A.	10.2 feet
sill ($C_{(2)}$)	N.A.	0.71
GRID C (1-foot scale)		
nugget ($C_{(0)}$)	0.16	0.165
range ($r_{(1)}$)	2.1 feet	2.1 feet
sill ($C_{(1)}$)	0.22	0.34
GRID D (1-inch scale)		
nugget ($C_{(0)}$)	0.26	0.35
range ($r_{(1)}$)	9.0 inches	2.0 inches
sill ($C_{(1)}$)	0.42	0.57

CONCLUSIONS

Analysis of permeability distributions (ignoring fractures) in this single shallowing upward sequence of the San Andres Formation reveals certain trends:

1. A generally low-permeability (<10 md), mud-dominated facies is overlain by a region of higher permeabilities (<10 md to <100 md). Streaks of higher permeability (>100 md) in the upper region are not continuous at small (1—ft to 1—in.) scales.
2. An inherent randomness (heterogeneity) of the permeability was observed at all linear scales covered in this study, from inches to hundreds of feet.
3. The analysis of horizontal and vertical variograms supported the visual observations of the existence of continuous heterogeneity across the range of scales.
4. The distribution of permeability within genetically defined depositional facies reflects the correlation range and mean permeabilities based on the fabric textures of the facies.
5. The heightened degree of heterogeneity at the small (inch-spaced) scale of investigation in this study is an indication that more information is required for determination of the controls of permeabilities at dimensions of less than a square foot. Heterogeneities within the generally highly permeable bar-crest facies indicate that values do vary widely within the space of an inch, creating low-permeability baffles and high-permeability conduits. Small-scale continuity and prevalence of the ocurrence within a formation can be most significant in determining the capacity of a reservoir to retain trapped fluids.
6. The application of power-law theory to the variogram databased on linear-scale samples produced a result for the fractal codimension that was an order of magnitude below the range proposed by other researchers for natural phenomena.

This study shows that it is reasonable to accept the conclusions of anisotropy and the scale dependence of the permeability, at least for this particular shallowing-upward parasequence of the upper San Andres Formation.

ACKNOWLEDGMENTS

We appreciate the reviews of Dr. Brenda Kirkland-George and Mr. Andy Czebieniak on earlier versions of this manuscript. This study is part of an integrated research effort carried out by a team of geoscientists in the Bureau of Economic Geology's Reservoir Characterization Laboratory. Numerous individuals have contributed, including G. E. Fogg,

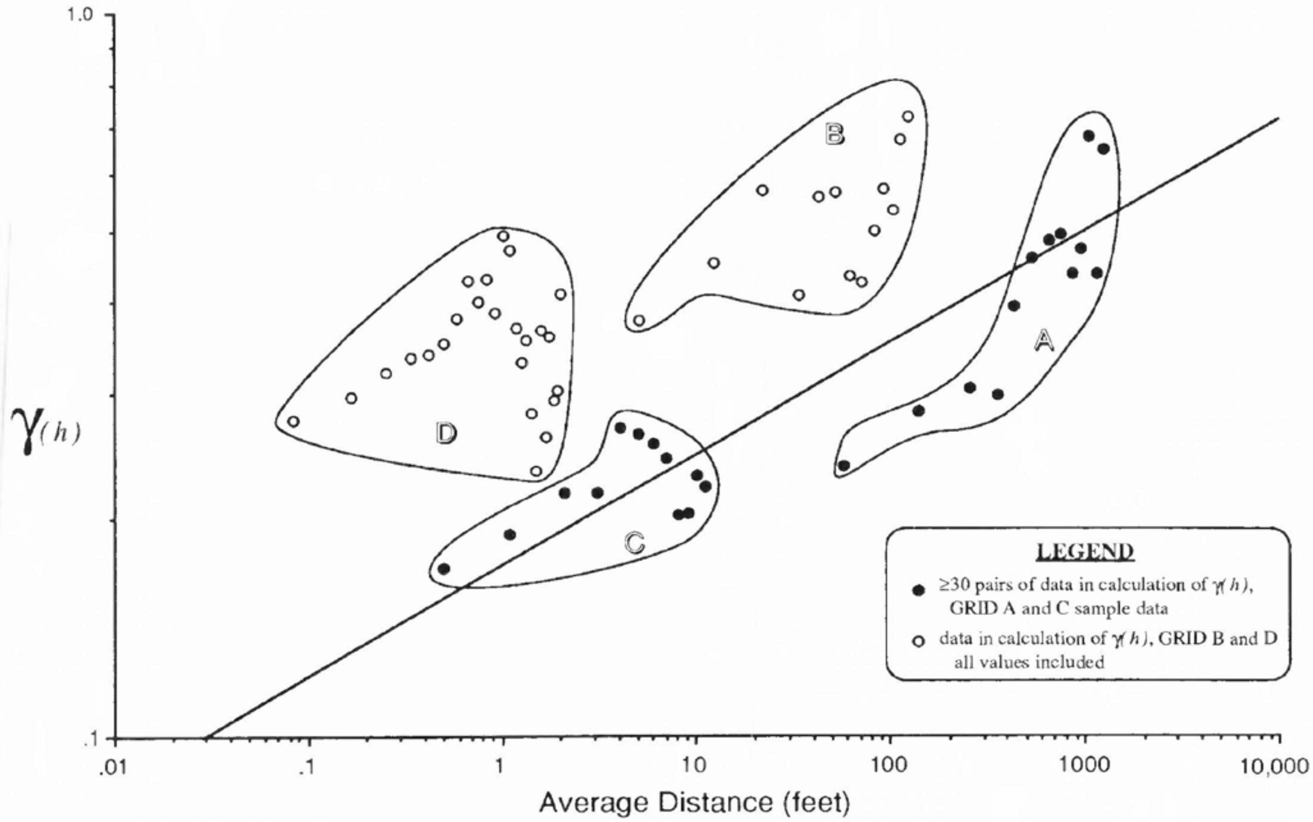

FIGURE 5. Superpositioned postings of variograms from scale-based grid samples plotted on log-axes. Best-fit line drawn through significant variogram calculations (greater than 30 data pairs per calculation of g(h) for GRIDs A and C samples). Power-law variogram parameters: slope = 0.155; y-intercept = –0.761; coefficient of correlation (R2) = 0.824.

H. S. Nance, E. Kasap, S. D. Hovorka, W. M. Fitchen, M. A. Ferris and F. Wang. Funding for this project was from industry sponsors Agip, Amoco, ARCO, British Petroleum, Chevron, Conoco, Exxon USA and Exxon Production Research, Fina, JNOC, Marathon, Mobil, Phillips, Shell, Texaco, Total and Unocal. The Department of Energy supplied matching funds for portions of this research under ANNEX I to DE-FG22-89BC14403 and DE-AC22-89BC14470. We also acknowledge the U.S. Forest Service and in particular Jeanie Milburn, for helpful cooperation. Roger Reisch of the National Park Service is also thanked for his hospitality. Manuscript preparation was supported by the Owen-Coates Fund of The Geology Foundation, The University of Texas at Austin. Rosemary Brant assisted in editing the manuscript.

REFERENCES

Chandler, M. A., Kocurek, G., Goggin, D. J. and Lake, L. W., 1989, Effects of stratigraphic heterogeneity on permeability in eolian sandstone sequence, Page Sandstone, northern Arizona: American Assocociation of Petroleum Geologists Bulletin, v. 73, p. 658-668.

Dagan, G., 1986, Statistical theory of ground water flow and transport: pore to laboratory, laboratory to formation and formation to regional scale: Water Resources: Research, v. 22, p. 120S-134S.

Davis, J. M. and Phillips, F. M., 1990, A quantitative study of heterogeneity: Sierra Ladrones Formation, central New Mexico; *in* Motyaner, G., ed., Transport and mass exchange processes in sand and thermal aquifers: field and modeling studies, Atomic Energy of Canada, Ltd., Chalk River, Ontario, p. 318-341.

Dykstra, H. and Parson, R. L., 1950, The prediction of oil recovery by water flood; *in* Secondary recovery of oil in the United States (2nd ed.), American Petroleum Institute, p. 160-174.

Eijpe, R. and Weber, K. J., 1971, Mini-permeameters for consolidated rock and unconsolidated sand: American Association of Petroleum Geologists Bulletin, v. 55, p. 307-309.

Ferris, M. A., 1993, Distribution of permeability patterns—upper San Andres Formation outcrop, Guadalupe Mountains, New Mexico [M.A. thesis]: Austin, University of Texas, 184 p.

Fogg, G. E., 1986, Stochastic analysis of aquifer interconnectedness with a test case in the Wilcox Group, east Texas [Ph. D. dissertation]: Austin, University of Texas, 216 p.

Fu, L., Milliken, K. L. and Sharp, J. M. Jr., 1992, Permeability variations in liesegang-banded Breathitt Sandstone (Pennsylvanian)—diagenetic controls: Geological Society of America, Abstracts with Programs, v. 24, no. 7, p. 254.

Fuller, C. M. and Sharp, J. M., 1992, Permeability and fracture patterns in extrusive volcanic rocks: implications from the welded Santana Tuff, Trans-Pecos Texas: Geological Society of America Bulletin, v. 104, p. 1485-1496.

Galloway, W. E., Ewing, T. D., Garrett, C. M., Tyler, N. and Bebout, D. G., 1983, Atlas of major Texas oil reservoirs: Bureau of Economic Geology, University of Texas, Austin.

Gelhar, L. W., 1986, Stochastic subsurface hydrology from theory to applications: Water Resources Research, v. 22, p. 135S-145S.

Goggin, D. J., 1988, Geologically sensible modeling of the spatial distribution of permeability in eolian deposits: Page Sandstone (Jurassic), northern Arizona [Ph.D. dissertation]: Austin, University of Texas, 417 p.

Goggin, D. J., Thrasher, R. L. and Lake, L. W., 1988, A theoretical and experimental analysis of minipermeameter response including gas slippage and high velocity flow effects: In Situ, v. 12, nos. 1 and 2, p. 79-116.

Hayes, P. T., 1964, Geology of the Guadalupe Mountains, New Mexico: U.S. Geological Survey, Professional Paper 446, 69 p.

Hewett, T. A. and Behrens, R. A., 1990, Conditional simulation of reservoir heterogeneity with fractals: SPE Formation Evaluation (September), p. 217225.

Hinrichs, P. D., Lucia, F. J. and Mathis, R. L., 1986, Permeability distribution and reservoir continuity in Permian San Andres shelf carbonates, Guadalupe Mountains, New Mexico: Permian Basin/Society of Economic Paleontologists and Mineralogists, Publication 86-26, p. 26-36.

Kerans, C., Lucia, F. J., Senger, R. K., Fogg, G. E., Nance, H. S., Kasap, E. and Hovorka, S. D., 1991, Characterization of reservoir heterogeneity in carbonate-ramp systems, San Andres/Grayburg, Permian Basin: Reservoir Characterization Research Laboratory, Final Report, Bureau of Economic Geology, University of Texas at Austin, 245 p.

King, P., 1942, Permian of west Texas and southeastern New Mexico: American Association of Petroleum Geologists Publication, p. 229.

King, P. B., 1948, Geology of the southern Guadalupe Mountains: U.S. Geological Survey, Professional Paper 480, 185 p.

Kittridge, M. G., 1988, Analysis of aerial permeability variations, San Andres Formation (Guadalupian): Algerita Escarpment, Otero County, New Mexico [M.S. thesis]: Austin, University of Texas at Austin, 361 p.

Krige, D. G., 1951, A statistical approach to some basin mine valuation problems on the Witwatersrand: Journal of the Chemical, Metallurgical and Mineralogical Society of South Africa, v. 53, p. 47-70.

Leary, D. A., 1984, Diagenesis of the Permian (Guadalupian) San Andres and Grayburg formations, Central Basin platform, West Texas [M.S. thesis]: Austin, University of Texas, 129 p.

Lee, W. T. and Girty, G. H., 1909, The Manzano group of the Rio Grande Valley, New Mexico: U.S. Geological Survey, Bulletin 389, 141 p.

Mandelbrot, B. B., 1983, The fractal geometry of nature: W. H. Freeman & Co., 468 p.

Sarg, J. F. and Lehmann, P. J., 1986, Facies and stratigraphy of lower-upper San Andres shelf crest and outer shelf and lower Grayburg inner shelf: Society of Economic Paleontologists and Mineralogists, Permian Basin Section, Publication no. 86-25, p. 9-36.

Sharp, J. M. Jr., Fuller, C. M. and Smyth, R., 1993, Permeability-porosity variations and fracture patterns in tuffs; *in* Hydrogeology of hard rocks: Proceedings of 24th Congress, International Assocication of Hydrologists, Oslo, June 1993, in press.

Silver, B. A. and Todd, R. G., 1969, Permian cyclic strata, northern Midland and Delaware Basins, west Texas and southeastern New Mexico: American Association of Petroleum Geologists Bulletin, v. 53, p. 2223-2251.

Van Wagoner, J. C., Posamentier, H. W., Mitchum, R. M., Vail, P. R., Sarg, J. F., Loutit, T. S. and Hardenbol, J., 1988, An overview of the fundamentals of sequence stratigraphy and key definitions: Society of Economic Paleontologists and Mineralogists, Special Publication no. 42, p. 40-45.

Weber, K. J., 1986, How heterogeneity affects oil recovery; *in* Lake, L. W. and Carroll, H. B. Jr., eds., Reservoir characterization: U.S. Academic Press, p. 487-544.